Geochemistry and REE minerals of nepheline syenites from the Motzfeldt Centre, South Greenland

A. P. JONES[1]

Division of Geological and Planetary Sciences
California Institute of Technology, Pasadena, California 91125

AND L. M. LARSEN

Grønlands Geologiske Undersøgelse
Øster Voldgade 10, DK-1350, Copenhagen, Denmark

Abstract

Whole-rock analyses including the REE are given for nineteen samples from four of the six overlapping nepheline syenite intrusions which constitute the Proterozoic ($\sim$1310 ma) Motzfeldt Centre. Larvikite margins of one unit (SM5) are apparently related to the nepheline syenites by early fractionation of Ol + Pl followed by fractionation of Ol + Pl + Cpx ± Amph at current levels of exposure. Positive Eu-anomalies in the larvikites might be explained by large-scale incorporation of earlier Pl-rich cumulates. Low initial $^{87}Sr/^{86}Sr$ ratios imply a mantle source, and the most basic magma was a late alkali gabbro giant dike with plagioclase megacrysts. REE- and incompatible element-rich peralkaline lujavrites with large negative Eu-anomalies are late stage products of extreme fractionation. Electron probe analyses of REE in eudialyte confirm this mineral as the major host to Zr and REE in the lujavrites. Other REE-bearing minerals in the nepheline syenites are Ca–Na–Ce–Ti–Zr–Nb-silicates of the rinkite–møsandrite and låvenite series, with up to 22 wt.% RE-oxides; some may be related to metasomatic fluids which had geochemical signatures similar to the lujavrites.

Introduction

The Motzfeldt Centre is the older of four major centers of igneous activity which make up the Igaliko Complex of nepheline syenites (Emeleus and Harry, 1970). It is situated at the eastern end of the Proterozoic alkaline igneous Gardar Province of southern Greenland (Emeleus and Upton, 1976). The Motzfeldt Centre has a determined Rb/Sr (whole-rock) age of 1310±31 ma and an initial $^{87}Sr/^{86}Sr$ ratio near 0.702 (Blaxland et al., 1978). The Motzfeldt Centre covers an area of approximately 350 km^2 and is well exposed as a steeply dissected and glaciated 2000 m plateau. The mineralogy of the mafic silicates together with a brief outline of the geology has been given by Jones (1984).

In this paper we present new whole-rock geochemical data for major and trace elements including the rare earth elements (REE). In particular the REE are contained in a variety of minerals, some of which show evidence of metasomatism. These minerals are principally eudialyte and alkali-zircono-silicates of the rinkite-møsandrite and låvenite series, and to a lesser extent, apatite, zircon and

sphene. Electron probe analyses including the REE in several of these minerals are reported and discussed.

The Motzfeldt Centre is especially interesting because a late stage peralkaline magma, lujavrite, was developed. This provides a link between the bulk of silica-undersaturated syenite plutons in the Gardar and the unusual peralkaline Ilímaussaq Intrusion (Ferguson, 1964, 1970; Bailey et al., 1981; Sørenson, 1969). We suggest that incorporation of earlier feldspar-rich cumulates in addition to extensive crystal fractionation could have played an important role in the overall petrogenesis of the syenites.

Geology

The Motzfeldt Centre was formed by a series of overlapping intrusions emplaced by a combination of block stoping and 5-10 km radius ring fractures. The country rock is mostly gneiss, known as Julianehåb granite (Allart, 1973) and a sequence of supracrustal rocks including metasediments, agglomerates and lavas collectively called the Eriksfjord Formation (Emeleus and Upton, 1976). Metasomatized and altered relics of the supracrustal rocks form large foundered raft-like xenoliths within the syenites and measure up to several kilometers in length and a few hundred meters in thickness. Adjacent lavas in the supracrustal volcanic rocks, including the altered xenoliths, range from alkali basalts to phonolites and are possibly
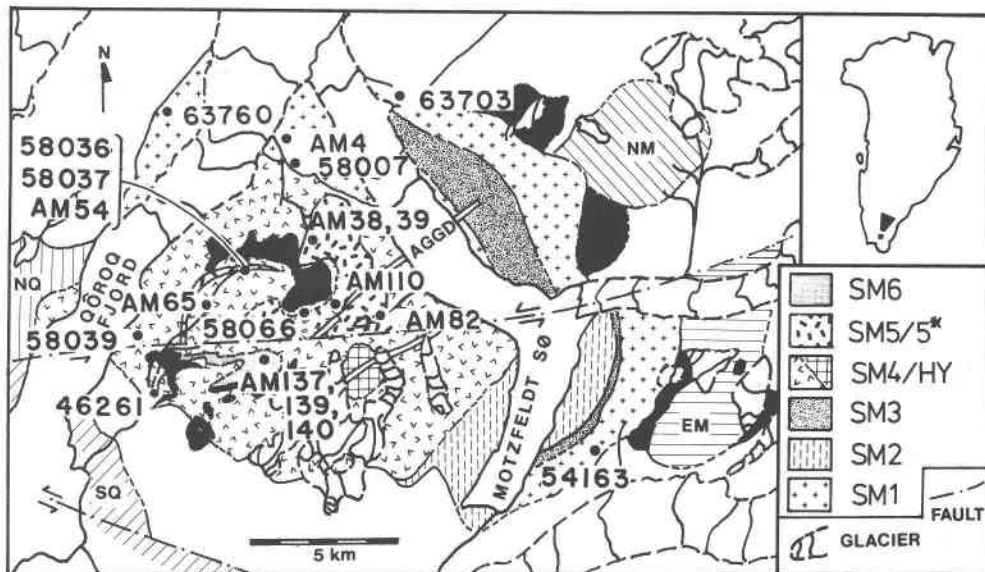
Fig. 1. Geology of the Motzfeldt Centre and location of samples used for whole-rock analyses in this study. Map after Jones (1984) with revised eastward extension to the major E–W fault after Tukiainen et al (1984). AGGD is alkali gabbro giant dike; EM = East Motzfeldt syenites; NM = North Motzfeldt syenites. Ornamentation, solid = supracrustal rocks. NQ = North Qôroq Centre (Chambers, 1976), SQ = South Qôroq Centre (Stephenson, 1976).

related to the Motzfeldt Centre itself (Jones, 1980). The center is cut by a major transcurrent E–W fault (The Flink's Dal Fault, Emeleus and Harry, 1970) which was shown to have a left lateral displacement of several kilometers (Jones, 1980) measured as 6 km to the east of the inland lake, Moztfeldt Sø (Tukiainen et al., 1984). The Geological Survey of Greenland is currently engaged in detailed investigations of several syenites and of radioactive mineralization in and around the center. There are six major syenite units, prefixed "SM" and numbered 1 to 6 in order of intrusion as indicated on the summary geological map in Figure 1. Future refinements to the geological boundaries of the syenite units are unlikely to affect the major conclusions of this paper, but might provide answers to some of the outstanding problems. A unit of late-stage lujavrites (SM6) and a sub-unit of cancrinite-rich roof-zone syenites (HY) were recognized subsequent to the work of Emeleus and Harry (1970) by Jones (1980). Unequivocal time relationships between units SM5 and SM6 have not been established, since they are separated by the Flink's Dal Fault. The center is cut by a regional swarm of ENE-trending trachytic dikes and a prominent alkali gabbro giant dike (AGGD) intruded in similar orientation. A few near-vertical carbonatitic and ultrabasic breccia pipes up to 200 m across also cut the center, but are not shown on Figure 1. The minor intrusions remain an attractive goal for future study and it is not known how they relate to the syenites. Thin discontinuous fluorite- and calcite-rich veins are found sporadically throughout the center and may provide clues to late stage metasomatic processes seen in some

structurally high levels. Pegmatites are sometimes associated with contacts between xenoliths and host syenites. Several pegmatites, microsyenite sills and altered limonite-rich shear zones in the center are enriched in radioactive minerals (Tukiainen et al., 1984).

The simplified geological map in Figure 1 shows the location of analyzed whole-rock samples (XRF) selected for additional REE determination by Instrumental Neutron Activation Analysis (INAA). The XRF analyses were obtained by Jones (1980) from which the following summary is largely extracted. The ranges of zoned mafic minerals, especially Fe/(Fe + Mg) and Na/(Na + Ca) in pyroxene, are related to the calculated normative differentiation index (D.I.) of the host rock. The D.I. was calculated after Thornton and Tuttle (1960) with the addition of normative acmite ($NaFe^3Si_2O_6$), which is important in the more fractionated syenites. Whole rock P and Ti decrease with increasing D.I. and increasing Fe/Mg, consistent with petrographic textures which indicate early crystallization of apatite and Ti-magnetite. Many of the syenites show cumulus textures in thin section and classic mineral banding, although rare, does occur in the center (Emeleus and Harry, 1970; Jones, 1980). Mineral compositions show normal zoning and combined trends which are the expected consequences of crystallization from increasingly fractionated syenite magmas. In addition to continuous zonation, the mafic minerals also show discontinuous zonation of the type pyroxene–amphibole–pyroxene (Jones, 1984). Bulk feldspar probe analyses are difficult to obtain because of perthitic textures and show a wide range in Ca-poor com-
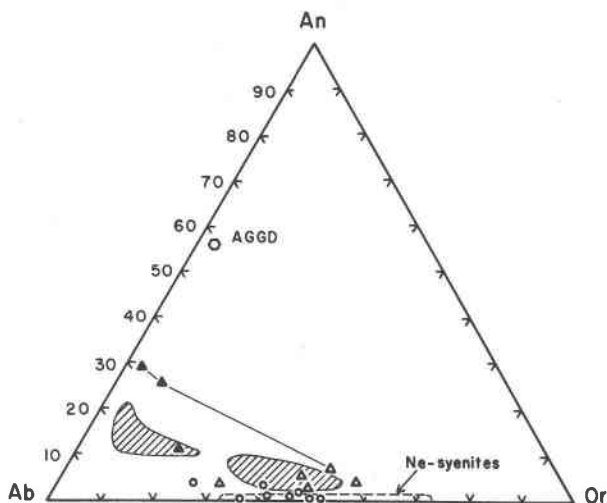
Fig. 2. Feldspar compositions (Ca–Na–K). Symbols: solid triangles = plagioclase cores in larvikites of SM5; open triangles = rims and normal feldspar from larvikitic syenites of SM5; open circles = feldspar from nepheline syenites of SM5; hexagon (AGGD) = plagioclase megacryst from alkali gabbro giant dike. Ruled areas are loci of feldspar (including plagioclase relics) from chilled facies of augite syenite at Ilímaussaq (Larsen, 1981). Range of feldspar compositions (bulk) of Motzfeldt syenites also indicated by dashed lines.

positions, illustrated in Figure 2. Calculated equilibration temperatures from nepheline compositions (Hamilton, 1961) range from 1050°C in the larvikites of unit SM5 to 750°C in the lujavrites of SM6, and some grains are normally zoned. Syenites from near the roof zones often show considerable replacement of nepheline by sodalite and/or cancrinite, coincident with peripheral enhancement of albite rims on perthite feldspars. Considerable subsolidus alkali exchange must have occurred, and calculations using the feldspar–nepheline geothermometer of Powell and Powell (1977) give a range of lower temperatures from 875 ±90 to 600±60°C for the majority of the unaltered syenites from Motzfeldt.

The current samples were chosen from the three largest syenite units (SM1, SM4, SM5) and the late stage lujavrites (SM6), in order to cover the range of fractionation and rock types present. Table 1 lists these samples and summarizes their rock types and special features; Table 1 also indicates which samples have been used in other publications. One sample from unit SM1 (63760) contains Nb-rich astrophyllite and has been hydrothermally altered. Unit SM5 is particularly useful since it grades from larvikites at its margin to eudialyte-bearing nepheline syenite at its interior. The mafic larvikites have weakly schillerized feldspar similar to Oslo region larvikites and are otherwise similar to augite syenite. Augite syenite occurs in association with many of the Gardar centers and is widely considered to be parental to many of the syenites (e.g., Upton, 1964; Emeleus and Upton, 1976). Feldspar in a partial ring

dike related to the margins of unit SM5 (SM5*) contains well defined plagioclase cores with irregular outlines and lamellar twinning abruptly terminated by mantles of crypt-operthitic alkali feldspar. Three reconnaissance microprobe analyses of the plagioclase show a range in composition from $Ab_{68}An_{28}Or_3$ to $Ab_{70}An_{11}Or_{19}$ and are plotted in the feldspar ternary in Figure 2. Similar, though slightly less calcic plagioclase cores ($<An_{20}$) occur in chilled facies of augite syenite from Ilímaussaq (Larsen, 1981). The bulk composition of the larvikite ring dike provides the best estimate of a basic magma available at Motzfeldt that was directly associated with the syenites (Table 2). However, the most basic rocks in the center, apart from the little studied carbonate plugs, are represented by the late AGGD (Fig. 1). The AGGD carries abundant plagioclase megacrysts ($\sim An_{56}Or_3$) and is similar to a Ti-rich alkali basalt in composition, with about 47 wt.% SiO_2 and 1–4% nepheline (Ne) in the CIPW norm at $Fe^3/Fe^2 = 0.1$ (Jones, 1980).

Analytical procedure

X-ray fluorescence analyses (XRF)

Original rock samples, typically 0.5 to 2.0 kg in size depending on grain size, were prepared by hand removal of weathered material, crushing in a jaw crusher and then milling in a tungsten carbide Tema disc mill. 100–200 g powdered samples were pressed into pellets and analyzed for selected major and trace elements using a Philips PW1212 automatic spectrometer with automatic sample loader at Durham University. Detailed procedures and standards are given in Jones (1980) and are available on request.

Instrumental neutron activation analyses (INAA)

Samples of 300–500 mg powder were irradiated for 3 hours at Risø National Laboratory, Denmark, in a reactor with a neutron flux of 4.5×10^{13} n/cm²/sec. The samples were arranged in batches of four unknowns and one pure Fe_2O_3 comparator, following the procedure of Girardi et al (1965). The counting was performed with a multichannel analyzer fitted with a Ge (Li) detector in two rounds; first after a cooling time of 7–8 days for 20–30 minutes, and second after a cooling time of 42–50 days for 80–120 minutes. The results were processed by computer using the program ARGON written by R. Gwodz, Copenhagen. This procedure identified peaks, performed interference correlations, and calculated concentrations. The results from one typical standard are given in the footnote to Table 3.

Electron micropobe

Mineral analyses were all made with a Cambridge Geoscan Mk II electron microprobe at Durham University. Major and minor elements were analyzed using analytical methods outlined in Jones (1984). Alkali-rich minerals such as feldspars, were analyzed with a defocussed beam of approximately 20 μm diameter. Special conditions for the REE, which were analyzed separately, followed procedures written by A. Peckett (given in Jones, 1980) and are briefly outlined here. An accelerating voltage of 20 kV, probe current of 80 nA as measured with a Faraday Cage in standard block, and LIF analyzing crystal in conjugation with a gas-glow proportional counter was used. A background was calculated based on average atomic number (Z) of the specimen, as scaled to absolute backgrounds measured on SiO_2, $NaNbO_3$ and SnO_2 which have a large range in Z. Collimating slits in front of the

Table 1. Rock samples analyzed

Unit	Sample	Rock type	Special features	Mafic minerals analyzed[a]
SM1	63703	syenite		AMPH
	AM4	nepheline syenite	Zr-rich aegirine	
	63760	syenite	Nb-rich astrophyllite	AMPH
	58007[b]	nepheline syenite		
	54163[b]			
SM4	58039[c]	nepheline syenite	olivine-bearing	AMPH
	58066	nepheline syenite		AMPH, AENIG
	AM65	nepheline syenite	intercumulus amphibole	
SM5	58036	larvikite ring dyke	plagioclase relics	OL
	58037	larvikite ring dyke	plagioclase relics	MICA
	AM54	larvikite ring dyke	plagioclase relics	
	AM39	larvikitic margin	olivine-rich	CPX, OL
	AM38	larvikitic margin	olivine-rich	CPX, OL
	AM110	nepheline syenite		CPX
	AM82	nepheline syenite	cumulus eudialyte(rare)	AENIG
SM6	AM139	white lujavrite		
	46261	dark lujavrite	eudialyte phenocrysts	
	AM137	white lujavrite	eudialyte-poor	
	AM140	white lujavrite		AMPH

[a]Mafic silicate analyses given in Jones (1984) for AMPH = amphibole, OL = olivine, CPX = clinopyroxene, AENIG = aenigmatite and MICA as indicated.

[b]whole rock sample not analysed for major elements but believed similar to 58007.

[c]Rb and Sr data given in Blaxland et al (1978)

Samples from each unit arranged with increasing D.I. downwards (see Table 2).

5-digit numbers are GGU (Greenland Geological Survey); AM-prefixes are from A.P.Jones.

Table 2. Whole-rock major element analyses (wt.%)

Unit	SM1				SM4			SM5							SM6			
Sample no:	63703	AM4	63760	58007	58039	58066	AM65	58036[a]	58037[a]	AM54[a]	AM39[a]	AM38	AM110	AM82	AM139	46261	AM137	AM140
SiO_2	60.98	56.51	63.69	58.27	54.77	54.85	56.27	51.10	51.87	53.44	49.73	55.95	57.24	57.93	54.04	56.97	55.69	58.07
TiO_2	0.88	0.36	0.22	0.31	0.91	0.88	0.09	2.47	2.30	2.26	1.58	1.58	0.34	0.34	0.37	0.02	0.16	0.07
Al_2O_3	16.55	20.51	16.48	20.14	18.99	19.30	21.55	15.82	15.96	15.77	16.14	17.97	20.22	20.66	16.68	18.72	19.47	21.29
Fe_2O_3			3.10								0.00	0.28		0.48	10.25	7.42	5.03	
$FeO*$	4.47	5.06	3.05	4.09	7.93	6.54	2.67	10.87	9.54	9.46	12.31	6.70	4.30	2.91	1.48	1.39	1.26	2.31
MnO	0.19	0.18	0.21	0.17	0.30	0.28	0.17	0.29	0.25	0.25	0.51	0.21	0.20	0.14	0.37	0.17	0.27	0.30
MgO	0.67	0.60	0.08	0.29	0.87	0.93	0.04	2.72	2.50	1.73	2.43	1.21	0.44	0.30	0.48	0.03	0.03	0.18
CaO	4.32	1.45	0.57	1.10	2.14	2.18	1.12	5.65	6.40	5.26	4.15	3.43	1.03	0.92	0.99	0.75	0.92	0.35
Na_2O	5.58	8.06	6.41	8.00	7.35	7.72	10.50	4.38	4.53	5.24	5.99	6.00	9.11	8.74	10.92	10.55	9.40	10.70
K_2O	6.27	5.94	5.50	6.28	5.46	5.57	6.24	3.92	3.70	4.34	4.51	4.67	5.80	6.28	3.61	3.96	5.15	4.85
P_2O_5	0.24	0.11	0.02	0.16	0.25	0.62	0.07	1.86	2.01	1.30	1.43	1.20	0.14	0.13	0.04	0.02	0.11	0.03
H_2O			0.36								0.74	0.86		0.47	0.94	0.06	2.51	
SUM	100.15	98.78	99.69	98.81	98.97	98.87	98.72	99.08	99.06	99.79	99.92	98.92	98.82	99.30	100.17	100.06	100.00	98.15
Na/(Na+K)	0.57	0.67	0.64	0.66	0.67	0.68	0.72	0.63	0.65	0.65	0.67	0.66	0.70	0.68	0.82	0.80	0.73	0.77
(Na+K)/Al	0.96	0.96	1.00	0.99	0.94	0.97	1.12	0.72	0.72	0.84	0.91	0.83	1.05	1.02	1.30	1.16	1.08	1.07
NORM Ne(Qz)	1.3	19.1	(4.3)	16.6	16.0	18.4	30.0	1.5	1.0	5.1	13.5	3.6	22.8	22.5	16.8	20.2	16.9	24.3
D.I.	82.8	88.1	91.5	91.7	80.8	83.5	89.0	59.4	59.8	66.2	66.6	76.0	87.9	90.7	73.9	82.2	90.8	93.0

Note : - *total iron where Fe_2O_3 not determined. Analyses arranged in increasing order of differentiation index (D.I.) for each unit. [a]samples from ring dyke and marginal syenite containing plagioclase relics. All analyses by XRF of pressed powder pellets at Durham University, except H_2O and Fe_2O_3 by titration. Average Fe3/Fe2 values for NORM calculations obtained for each unit were; SM1 = 1.8, SM4 = 0.66, SM5 = 0.05 (58036, 58037, AM54) and 0.30 (the rest), SM6 = 5.6.

Table 3. Whole-rock trace element analyses (ppm)

Unit Sample	63703	AM4	63760	58007	54163	58039	58066	AM65	58036	58037	AM54	AM39	AM38	AM110	AM82	AM139	46261	AM137	AM140
Ba	2142	568	155	708	586	1254	898	57	4618	5143	2685	1702	3766	433	878	190	40	250	263
Rb	107	227	422	251	200	232	185	280	41	37	89	122	84	222	201	313	357	482	542
Sr	769	280	71	284	131	413	472	65	1219	1601	872	841	1992	241	428	50	26	73	56
La	53.3	86.3	195	129	120	119	167	211	72.2	60.4	82.7	196	104	83.1	67.1	270	352	339	263
Ce	133	199	414	274	273	290	397	444	161	122	181	430	215	173	142	603	667	577	460
Nd	48.7	69.9	120	80.4	98.5	111	137	163	82.7	63.7	63.0	195	99.1	59.2	48.3	219	225	199	184
Sm	8.36	11.0	17.3	12.8	15.4	15.1	17.5	26.4	15.0	11.5	14.2	28.8	15.0	9.95	8.37	29.4	45.1	27.2	24.3
Eu	5.09	1.60	1.27	1.63	1.58	2.16	5.00	2.15	6.84	6.60	6.07	6.63	8.33	2.45	2.90	1.96	2.52	1.87	1.82
Tb	0.77	1.23	1.55	1.57	1.82	1.77	2.06	3.12	1.70	0.82	1.68	2.75	1.28	1.35	0.96	3.19	8.15	3.30	4.78
Yb	1.61	3.24	6.23	3.27	2.57	4.73	5.01	8.68	2.12	1.91	3.44	5.52	2.11	5.35	2.61	8.13	34.6	(3.6)	12.3
Lu	0.25	0.48	0.91	0.48	0.38	0.75	0.86	1.17	0.32	0.27	0.56	0.80	0.29	0.78	0.41	1.22	4.74	1.01	1.68
Y	24	33	58	30		42	52	98	33	29	47	62	32	37	26	86	251	108	127
Th	3.4	10.9	22.6	13.1	9.7	11.2	19.6	25.9	2.0	2.3	5.1	10.1	3.6	7.9	10.0	36.3	5.8	186	91.4
U	4.0	2.6	113	8.9	7.3	6.0	4.0	6.9	2.7	7.0	2.0	8.2	6.7	10.0	4.5	27	21	58	21
Zr	308	870	668	634	406	808	748	519	176	180	448	783	282	1324	707	2005	4230	1040	2449
Hf	7.4	20	28	18	10	24	21	14	5.0	5.2	13	23	7.3	41	16	53	147	26	60
Nb	73	205	1589[a]	176		267	177	117	46	42	102	224	82	271	154	608	478	688	595
Ta	4.8	12	235[a]	12	7.8	16	13	6.6	3.6	2.4	7.5	16	6.5	26	10	27	79	12	34
Sc	11	1.2	1.6	1.5	1.9	8.0	7.5	0.6	25	35	51	9.5	6.6	3.2	2.3	3.6	0.3	0.9	0.3
Zn	122	123	454	158	94.3	263	176	91.5	297		337	287	147	107	84.5	546	132	789	682
Pb	23	10	58	19		13		24	2		23	34	14	17	27	51	48	57	58
Eu/Eu*	2.33	0.52	0.28	0.44	0.36	0.50	0.99	0.28	1.61	2.38	1.49	0.91	2.15	0.81	1.22	0.24	0.17	0.24	0.22
Ce/Yb	82.6	61.4	66.5	83.8	106.2	61.3	79.2	51.2	75.9	63.9	52.6	77.9	101.9	32.3	54.4	74.2	19.3	161.6	37.4
Zr/Hf	41.6	43.5	23.9	35.2	40.6	33.6	35.6	37.1	35.2	34.6	34.5	34.0	38.6	32.3	44.2	37.8	28.8	40.0	40.8
Hf/Ta	1.54	1.67	0.12	1.50	1.28	1.50	1.60	2.12	1.39	2.17	1.73	1.44	1.12	1.58	1.60	1.96	1.86	2.17	1.76
Nb/Ta	15.2	17.1	6.8	14.7		16.7	21.3	17.7	12.8	17.5	13.6	14.0	12.6	10.4	15.4	22.5	6.1	57.3	17.5

Note: – Ba Rb Sr Y Pb Zr and Nb analyzed by XRF at Durham University, the remainder were analyzed at Risø (Denmark) by INA; see text for details. INA standard results for CRPG-BR versus international reference in brackets;– Sc 22.2 (26.2), Zn 55.8 (50), La 82.9 (80), Ce 140 (140), Nd 52.5 (60), Sm 10.9 (12), Eu 3.52 (3.7) Tb 1.22 (1.1), Yb .815 (2.0), Lu .194 (.13–.27), Th 9.77 (12).

[a] Sample contains Nb-rich astrophyllite.

detector gave a resolution of approximately 4' arc, or 5 eV for the region of interest, but several overlapping lines could not be avoided, despite selection of Lα or Lβ lines, and an interference matrix was established by experiment. Thus, interferences among the REE were removed iteratively and finally conventional ZAF corrections were applied to the complete analysis. Errors become particularly serious at the low levels of heavy REE (especially Ho, Tm, Lu). Subsequent inspection of the results showed residual interference from Mn on Dy, which was discarded on Mn-rich minerals, and Eu represents a maximum since a small contribution from Pr or Sm at the EuLβ peak used could not be avoided.

Whole rock geochemistry

Major elements

Whole rock major element analyses are given in Table 2 and include Fe_2O_3 and H_2O for several samples. Calculated differentiation indices (D.I.) from the CIPW norm are based on the D.I. of Thornton and Tuttle (1960) plus normative acmite. D.I. values range from 59 to 93 (Table 2) and on this basis samples can be conveniently referred to as more- or less-fractionated. The syenites all contain normative nepheline (Ne) which, apart from the low values, corresponds more or less with modal proportions estimated from hand specimens and thin sections. One obvious exception is sample 63760 of unit SM1 which has normative quartz (Qz) at the $Fe^{3+}/(Fe^{2+} + Fe^{3+})$ value used.

This sample has been hydrothermally altered and contains neither free quartz nor nepheline. The peralkalinity index increases with D.I. such that the fractionated samples of each unit are peralkaline with (Na + K)/Al > 1, as are all samples of unit SM6 (lujavrites). The ratio Na/(Na + K) varies little within each unit, and the total range for all of the units is from 0.57 to 0.82.

A plot of the major oxides versus SiO_2 (not illustrated) shows the same features exhibited by the larger data base (90 additional samples) of Jones (1980). Such Harker variation diagrams are of limited use, due to the restricted range of SiO_2 in most units, except for SM5. The latter unit shows simple trends of decreasing MgO, FeO, P_2O_5 and TiO_2 with increasing SiO_2; CaO decreases after a hiatus near 52 wt.% SiO_2, and Al_2O_3 remains nearly constant to approximately 53 wt.% SiO_2, above which it increases. Apart from the two silica-rich samples of SM1, all the major oxides of the other syenites cluster loosely around the SM5 data in the range 54–58 wt.% SiO_2.

Minor elements

Table 3 gives analyses for 8 REE and 13 other minor elements for the 19 samples. Blank spaces in Table 3 are values below detection limits and the precision for each element can be approximately inferred from the number of significant figures quoted. Ba, Sr and Sc decrease by approximately two orders of magnitude from their highest
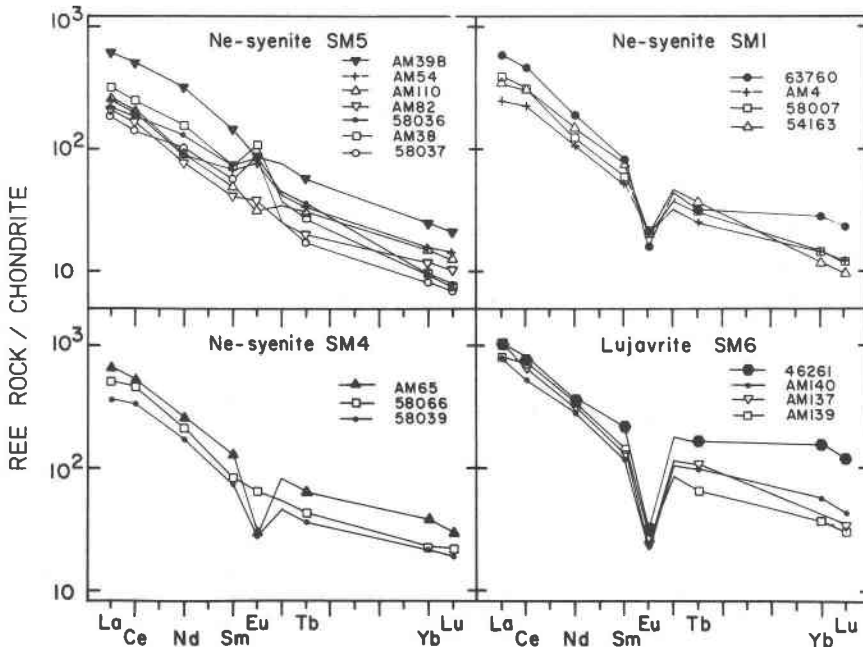
Fig. 3. Whole-rock REE normalized to chondrite abundances (Nakamura, 1974) plotted on log scale.

values in the least-fractionated samples and have their lowest values in the lujavrites of SM6. Zn decreases with increasing D.I. in each unit but is highest again in unit SM6 and the hydrothermally altered sample of unit SM1 (63760). Zr, Hf, Nb and Ta are highest in unit SM6, although these elements do not increase systematically with D.I. or any other obvious element. The average Zr/Hf ratio is 37 ($\pm$4.2, 2σ) for the nineteen samples, excluding 63760 which has Zr/Hf = 23.9. The ratios Hf/Ta and Nb/Ta are reasonably constant at approximately 1.5 and 15 respectively, for most samples except 63760 which contains Nb-rich astrophyllite. The Nb/Ta ratio is also particularly variable in SM6 which contains pyrochlore.

REE

The REE whole-rock data are given in Table 3 and were normalized using the customary chondrite abundances of Nakamura (1974). The normalized REE (REE$_N$) are plotted for each syenite unit in Figure 3. Recent revisions of chondritic abundances, such as those employed by Davis et al. (1982) would increase the REE$_N$ levels overall, but cause only minor differences in their relative distributions. For descriptive purposes, a distinction is made between least fractionated and fractionated samples of each unit, based on D.I. This does not require that all samples are related by crystal fractionation, but is a useful mechanism for discussion.

As illustrated in Figure 3, all of the samples are steeply light REE-enriched, with high positive values of Ce/Yb and most have a Eu-anomaly. The Eu-anomaly may be negative or positive and varies greatly in relative size. It can be

expressed numerically as Eu/Eu* where Eu* is the expected Eu interpolated from the two adjacent REE (in this case Sm and Tb) assuming no Eu-anomaly. The least fractionated sample grouped with unit SM1 (63703) has the lowest REE and a prominent positive Eu-anomaly. This is very different from other samples of SM1 and is now thought to belong to an earlier syenite that predates SM1 (Tukiainen, pers. comm. 1984) and is excluded from Figure 3. All samples from SM1 have a negative Eu-anomaly which shows some correlation between its size (Eu/Eu* < 1) and the level of total REE. The most fractionated sample of SM1 contains the most REE, except for Eu, and is the silica-rich hydrothermally altered 63760. The three samples of unit SM4 have similar REE levels (Fig. 3) despite their large geographical separation (Fig. 1) and measured range in major element chemistry (Table 2). One sample has a negligible Eu anomaly and two have substantial negative Eu-anomalies. By a narrow margin, unit SM5 has the overall lowest REE levels and five of the seven samples have positive Eu-anomalies of varying size. The latter include three samples from the earliest marginal larvikite (SM5* partial ring dike, Table 1) which contain plagioclase cores to alkali feldspars. There is a suggestion that the three samples of SM5 with small Eu-anomalies (AM82, AM110, AM54) have a kinked REE pattern, which is steep from La to Sm but flatter in the heavy REE from Tb to Lu; the same is true for two samples of SM1. This really requires a closer spread of analyzed heavy REE between Tb and Lu to analyze further. Unit SM6 lujavrites have the highest REE levels, and these become less steep (Ce/Yb from 162 to 19, Table 3) with increasing total REE
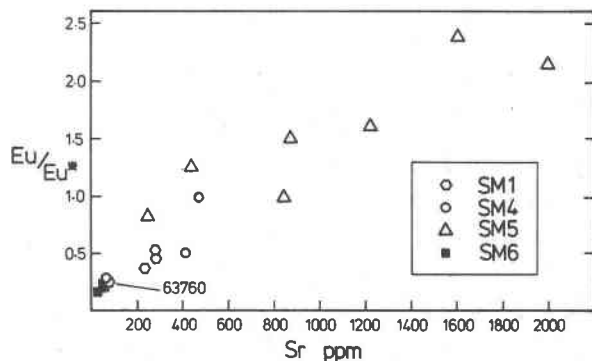
Fig. 4. Eu/Eu* versus Sr (whole-rock). Eu* is straight line interpolated value between Sm and Tb, assuming no Eu-anomaly. The data show good correlation between decreasing Eu/Eu* and Sr. Sample 63760 indicated for SM1 is hydrothermally altered syenite.

abundances. The one dark lujavrite (46261) typified by eudialyte phenocrysts (Fig. 5) has the highest REE measured, and the pattern is more obviously kinked. Comparison of all the patterns in Figure 3 shows that of the three syenite units analyzed, SM1 and SM4 have the closest similarity to unit SM6; this is important when considering the petrogenesis of the lujavrites. Thus, there is a reasonable overlap between the highest samples of SM1 (63760) and SM4 (AM65) and the lowest REE sample of the lujavrites (AM140).

There is an interesting relationship between the Eu-anomaly and Sr for all the syenites, shown in Figure 4. Eu/Eu* decreases uniformly with decreasing Sr, with Eu/Eu* > 1 in Sr-rich larvikites to Eu/Eu* < 1 (i.e., negative Eu-anomaly) in Sr-poorer nepheline syenites of SM5. A similar relationship is shown by the other syenites, with lowest values of Eu/Eu* representing the largest negative Eu-anomalies found in Sr-deficient lujavrites of SM6. Similar correlations are found in analogous plots of Eu/Eu* versus Ba and Ca (not shown). This is important since Ba, Sr, Ca and P all decrease with increasing D.I. and SiO_2, and both apatite and plagioclase feldspar are common in the early larvikites of SM5. Their relative roles might be expected to directly influence Eu-anomalies and are discussed in a later section.

REE-bearing minerals

The REE are present in a number of different minor and accessory minerals in the Motzfeldt syenites and some of these increased or diminished in importance possibly in response to changing compositions of host magmas. Some may have been replaced during circulation of metasomatic fluids. A number of these minerals have been analyzed by electron microprobe and representative analyses are given in Table 4. Examples of their textural relationships are illustrated in Figure 5. Apatite, which is characteristically light REE-rich (e.g., Henderson, 1980; Larsen, 1979) and

usually has a negative Eu-anomaly (Watson and Green, 1981) is common in the early and mafic syenites, such as the larvikites of SM5, but is largely absent from the more fractionated syenites. This is reflected in whole-rock P_2O_5 values in Table 2, which decrease with increasing D.I. Zircon, which has a heavy REE-dominated pattern (e.g., Exley, 1980) is common in many of the nepheline-poor syenites. Euhedral zircon forms up to 10% of the mode in rare mafic bands with melanite garnet and euhedral pyrochlore in unit SM1 (Jones, 1980). Zirconium also occurs in solid solution in late-stage aegirine, with up to 7.0 wt.% ZrO_2 in syenites of unit SM3 (Jones and Peckett, 1980). In all analyzed aegirine, however, REE levels were below detection (50 to 100 ppm element) even in the most Zr-rich aegirine. More importantly, Zr occurs in the mineral eudialyte, $Na_4(Ce,Ce,Fe)_2ZrSi_6O_{17}(OH,F,Cl)_2$ in the most fractionated syenites and this mineral contains up to 7.0 wt.% RE-oxides (RE_2O_3, Table 4). Eudialyte occurs as an essential mineral in the lujavrites (SM6) where its habit of phenocryst or interstitial texture (Fig. 5) distinguishes dark lujavrite from white lujavrite (Jones, 1980). Eudialyte from unit SM4 (AM49, Fig. 6) is light REE-enriched and eudialyte from white lujavrite (Table 4, AM159) contains the highest RE_2O_3. It should be emphasized that the heavy REE measured by electron probe are close to theoretical detection limits and have serious limitations in precision (circa ±10% or worse). Nevertheless, the analyzed eudialytes have a kinked REE pattern which is steep from La to Nd and flatter from Sm to Yb (Fig. 6). Y generally behaves like Ho, a heavy REE (e.g., Jones and Ekambaram, 1985) and measured values for the two eudialyte grains in Table 4 have chondrite-normalized abundances in the range $3–7 × 10^3$, in agreement with the heavy REE shown in Figure 6. This kinked pattern for eudialyte compares favorably with the whole-rock REE for dark lujavrite (46261) which is similarly kinked (Fig. 3) and shown for comparison in Figure 6. REE in the dark lujavrite might reasonably be expected to reflect the REE-bearing eudialyte. In detail, the ratios Zr/Ce and Zr/Yb for eudialyte and whole rock do not agree very closely. This is probably because of additional Zr and REE mineral hosts in the lujavrites including alteration products of eudialyte. Whole rock Zr abundances for the dark lujavrites (Table 3) agree with modal estimates of circa 5% eudialyte phenocrysts (i.e., 5% × 12.2 wt.% ZrO_2 = 4500 ppm Zr rock). Consequently, the REE are expected to be 2–3 times lower in unanalyzed interstitial eudialyte from white lujavrite, which has similar amounts of eudialyte but lower whole rock Zr. Much of the eudialyte in the lujavrites has been replaced by secondary hydrous minerals, including catapleiite $Na_2ZrSi_3O_9·2H_2O$ (Fig. 5). The same lujavrites show replacement of nepheline by cancrinite, fine-grained white mica (?Li-rich) and sodalite; coexisting feldspars of albite and microcline are uneffected. The evidence suggests some alteration by alkali-rich, Cl-bearing hydrous fluids, which might also have modified the REE, Zr/Ce and Zr/Yb rock ratios.

Anhedral sphene ($CaTiSiO_5$) is locally common as an
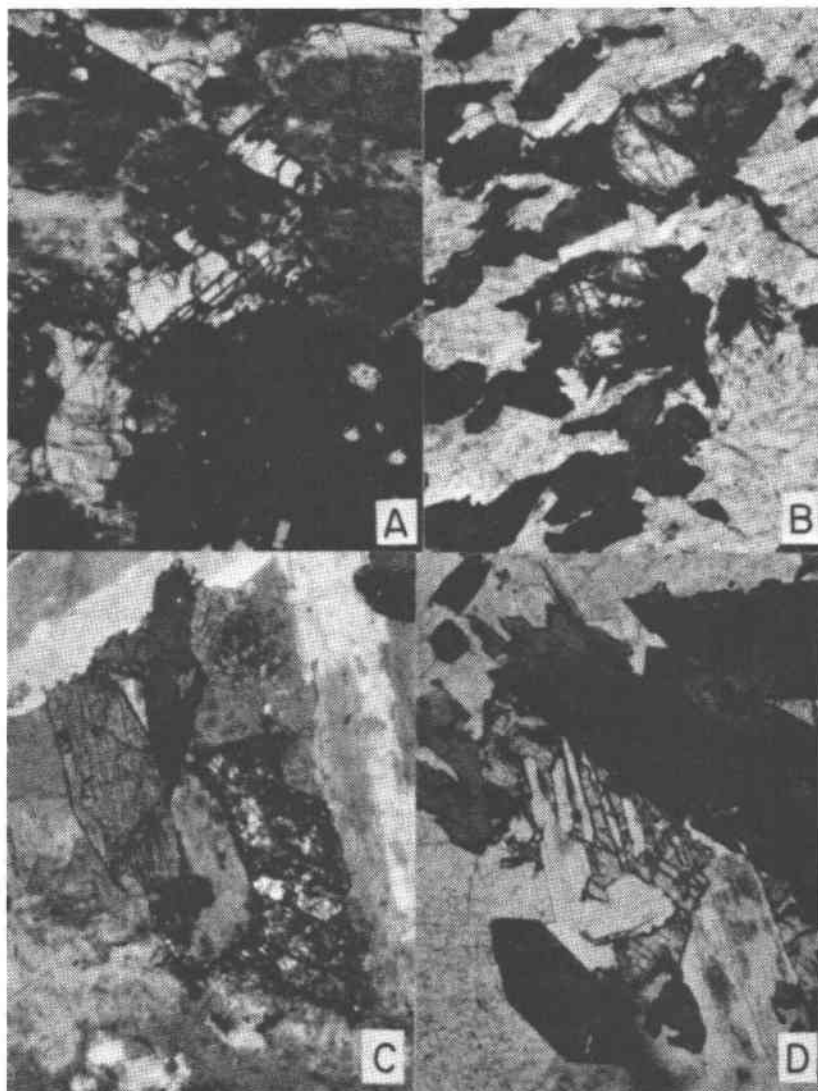
Fig. 5. Photomicrographs of typical accessory phases in the Motzfeldt syenites: all have width near 2 mm, all plane polarized light except (c) which has partly crossed polars. (a) Clear, well-cleaved (and parallel twinned, not shown) rinkite in center is interstitial to turbid alkali feldspar, clear nepheline and dark amphibole (AM7, unit SM4). (b) High relief and irregularly fractured phenocrysts of eudialyte (center and above center) with aegirine, nepheline, albite and microcline (various shades) in dark lujavrite (AM164, unit SM6). (c) High relief interstitial and partly altered eudialyte (just right of and below center) with aegirine blades (dark) in white lujavrites (AM138, unit SM6). (d) Moderate relief interstitial Mn-pectolite with good cleavage (near center) with albite (clear), microcline (turbid) and bladed aegirine (dark) in white lujavrite (AM139, unit SM6).

accessory mineral in the Motzfeldt syenites; although based on typical analytical totals near to 100%, it is not a major repository of REE. Sphene can be light REE-enriched in felsic rocks (e.g., Exley, 1980; Fleischer, 1978; Henderson, 1980). The majority of the Motzfeldt syenites contain no sphene but usually have accessory minerals of a variety of Ca–Na–Ce–Ti–Zr–Nb-silicates of the rinkite–møsandrite and låvenite series; these contain up to ~ 22 wt.% RE_2O_3 (Table 4). The same minerals are also

common in the adjacent North Qôroq Centre, where Chambers (1976) established a correlation between the abundance of rinkite and the degree of contamination of the syenites by metasomatized country rocks. These minerals are usually interstitial, or less commonly euhedral, and colorless to pale yellow; they are rarely visible in hand specimen. They often have anomalous birefringence and can have lamellar twinning superficially resembling plagioclase. Rinkite can be represented by the formula

Table 4. Electron probe analyses of accessory minerals (wt.%)

	1 sphene	2 zircon	3* lav	4* rink	5c* rink	5r* rink	6 lav	7* eud	8* eud	9 Mn-pect
Nb_2O_5	0.90	n.a.	2.63	2.66	3.01	1.61	13.50	1.74	2.47	n.a.
SiO_2	29.42	32.29	30.30	30.46	31.19	30.04	30.24	47.33	46.51	55.95
TiO_2	37.47	0.15	0.74	10.41	10.34	6.69	1.01	0.15	0.11	0.02
ZrO_2	0.20	66.13	17.13	1.47	6.26	9.16	15.09	12.52	12.21	
HfO_2		1.03								
Al_2O_3	0.64	0.05	0.01	5.03	1.38	0.19	0.08	0.18	0.73	0.11
Y_2O_3			1.9[a]	2.77	2.65	1.90		0.9[a]	1.5[a]	
La_2O_3			0.17	3.46	1.53	0.41		0.49	1.40	
Ce_2O_3			0.49	10.49	5.53	1.52		1.29	2.87	
Pr_2O_3			0.09	1.05	0.63	0.29		0.22	0.39	
Nd_2O_3			0.26	4.36	2.20	0.73		0.41	0.76	
Sm_2O_3			0.18	0.77	0.51	0.24		0.16	0.26	
Gd_2O_3			0.15	0.68	0.48	0.25		0.10	0.28	
Dy_2O_3			b	0.14	0.63	0.36		b	b	
Er_2O_3			0.13	0.27	0.28	0.24		0.12	0.20	
Yb_2O_3			0.07	0.15	0.25	0.21		0.06	0.26	
FeO	1.85	0.27	1.53	6.63	0.97	0.82	0.78	6.97	6.73	1.07
MnO	0.13	0.22	1.37	0.09	0.79	0.91	0.71	2.19	4.59	15.56
MgO	0.19	0.08	0.05	0.03	n.d.	n.d.	0.11	n.d.	n.d.	0.16
CaO	27.83	0.04	30.78	10.18	20.30	28.29	30.54	10.40	6.25	16.44
Na_2O	0.84	0.05	6.49	1.96	3.12	8.12	2.16	12.13	10.79	8.82
K_2O	0.03	0.02	0.02	0.15	0.21	0.08	n.d.	0.17	0.12	0.08
SUM	99.50	100.33	94.56	93.21	92.26	92.06	94.22	97.53	98.43	98.21

Note: – *REE patterns illustrated for these minerals in Fig. 6. 1 = AM81 interstitial sphene in coarse-grained ne-syenite (SM5). 2 = 63717 zircon core of euhedral grain (0.2 cm) in mafic banded syenite (SM3). 3 = AM51 ?lavenite interstitial grain in foyaite (SM4). 4 = AM81 yellow euhedral ?rinkite (0.3 cm) in coarse-grained ne-syenite (SM5). 5 = AM84 core (c) and rim (r) of yellow zoned ?rinkite euhadral grain (0.5 cm) in coarse-grained ne-syenite (SM5). 6 = 63725 Nb-rich ?lavenite interstitial grain (SM4). 7 = AM49 interstitial colorless eudialyte in foyaite (SM4). 8 = AM159 interstitial pale yellow eudialyte in white lujavrite (SM6). 9 = AM138 colorless to pale yellow/brown interstitial Mn-pectolite in white lujavrite (SM6).
[a]estimated from peak counts only. [b]serious inteference from Mn. n.d. = not detected.

(Ti,Nb,Zr)(Na,Ca)₃(Ca,Ce)₄– (Si₂O₇)₂(O,F)₄ (Galli and Alberti, 1971) and a typical example from Motzfeldt is shown in Figure 5. A more general formula for this family would be $XYZ_2OF(Si_2O_7)$ and a few representative (partial) analyses are given in Table 4. Recasting the cation proportions of seven such analyses assuming Si = 2.00 gave totals for (X + Y + Z) from 3.01 to 4.05, with cation totals varying from 7.91 to 9.25, indicating more than one mineral type. There is a chemical similarity between the rinkite/låvenite minerals and sphene (Table 4) considering the nearly constant SiO_2 and the common substitutions of Na, Nb and Zr for Ca and Ti seen in other minerals. Sphene and rinkite do in fact share some structural elements (P. B. Moore, pers. comm., 1984) and chemically rinkite represents an enriched variety of sphene. The notably fresh appearance of rinkite in some altered syenites with clouded feldspars and general petrographic textures hint at a possible metasomatic origin. Detailed electron probe analyses of the REE in rinkite are plotted in Figure 6. The larger crystals (>1 mm) are zoned from REE-rich cores to relatively REE-poor rims (Table 4).

Interpretation

Petrogenesis

The systematic variations shown by major elements between early mafic larvikites and evolved nepheline syenites of unit SM5 can be related either by fractional crystallization or partial melting. Using the most basic mineral compositions analyzed from the larvikites (Jones, 1984) the trends have been modelled (not shown) by early extraction of olivine (Ol) and plagioclase (Pl) in approximately equal proportions, followed by extraction of Ol + Pl with additional clinopyroxene (Cpx) with or without amphibole (Amph). Alternatively, successively derived partial melts would be in equilibrium with residues of Ol + Pl + Cpx ± Amph and Ol + Pl respectively. Olivine and clinopyroxene occur as phenocrysts or early formed crystals, and
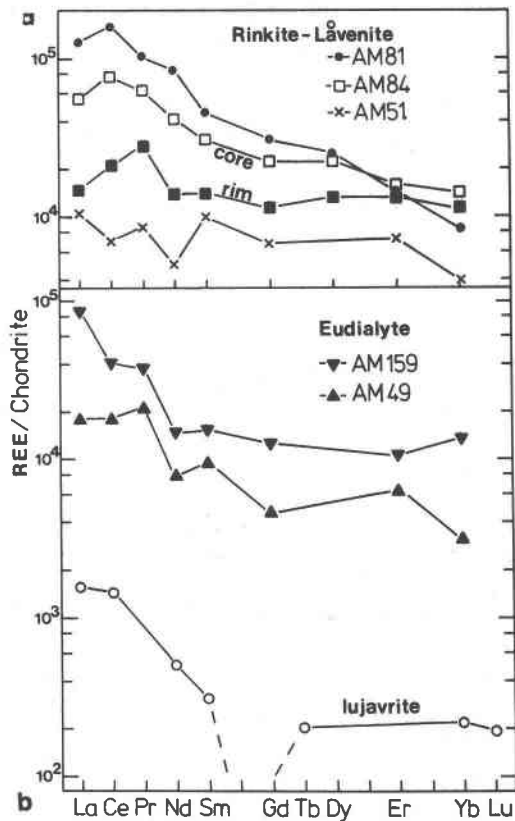
Fig. 6. Chondrite-normalized REE data for accessory minerals. (a) Rinkite-låvenite types including core and rim of zoned grain; (b) eudialyte from unit SM4 (AM49) and unit SM6 (AM159) showing kinked REE patterns (steep La to Sm, flatter Gd to Yb) which compare well with the whole-rock data for a lujavrite sample, which has eudialyte phenocrysts (46261, similar to illustration in Fig. 5 (b)).

subtraction of Cpx $\pm$ Amph above approximately $SiO_2 =$ 54 wt.% SiO_2 coincides with the transition from larvikites to nepheline syenites. This might be interpreted as a change from Ol + Pl controlled magmas in the ring dike to Ol + Pl + Cpx $\pm$ Amph in the main chamber at current exposure levels. We believe that the magmas are derived by crystal fractionation processes.

By analogy with unit SM5, the other syenite units of the Motzfeldt Centre are taken to have similar origins. This is supported by overlapping whole-rock and mineralogical trends (Jones, 1980, 1984) and field relations, although only SM5 is clearly associated with larvikitic magmas. Time intervals between overlapping intrusions were at least long enough to allow solidification. Rather similar fractionation schemes were deduced by Upton and Thomas (1980) for an important suite of transitional olivine basalts in the Late Gardar Younger Giant Dike Complex at Tugtutôq (YGDC). The Tugtutôq YGDC was related by relatively low pressure (crustal, < 10 kbar) Ol + Pl fractionation, and an even deeper level evolution apparently dominated by pyroxene and garnet. The Tugtutôq YGDC encompasses a larger compositional range than 8 preliminary analyses of the Motzfeldt AGGD, but their ultimate petrogenetic histories are undeniably similar. Even plagioclase megacrysts in the Motzfeldt AGGD and anorthosite inclusions in the Tugtutôq YGDC have similar compositions (An_{56}, An_{58-52}). These giant dikes tapped a magma source that may have been available in large quantities throughout the Gardar Period. Indeed they may have been directly related to the intrusive centers by dilation and subsequent ring fracture, as envisaged by Bridgwater and Harry (1968). The consistently low initial $^{87}Sr/^{86}Sr$ ratios are taken to imply a mantle source (Blaxland et al., 1978; Patchett et al., 1976) and preclude large scale involvement of the Julianehåb Granite (upper crust).

Eu-anomalies

The most fractionated syenites have the largest negative Eu-anomalies, there is a simple relationship for Eu/Eu* versus Sr (Fig. 4), and Sr decreases with increasing fractionation. Thus, large positive anomalies exist in the least-fractionated Sr-, Ba- and P-rich larvikites of SM5, which are considered to be related to the evolved nepheline syenites by crystal fractionation (section above). Similar positive Eu-anomalies exist in the Oslo region alkaline rocks, in most of the lardalites (nepheline-rich larvikites) and about half of the larvikites (Neumann, 1980), and their character and compositions are comparable to the larvikites of SM5. Neumann interpreted the Oslo samples with positive Eu-anomalies as cumulates, derived by a complex scheme of addition and subtraction of feldspar, apatite and femic minerals in specific proportions. A model involving separation of clinopyroxene, apatite and kaersutite was proposed to explain much smaller positive Eu-anomalies in anorthoclase phonolites from Ross Island (Sun and Hanson, 1971, p. 149). It is well established that the anorthite (Ca) component in feldspar exerts a strong preference

plagioclase is found in cores of alkali feldspars in the larvikites; amphibole only occurs as an interstitial mineral. Field relations show that the larvikitic margins gradually merge into nepheline syenites and occasional banding with cumulus textures is found in the nepheline syenites of SM5 (Emeleus and Harry, 1970). Plagioclase compositions used were constrained by relations between CaO, Al_2O_3 and SiO_2 to be at least as An-rich as the most calcic cores in the larvikites ($<An_{28}$) for the low silica part of the trends (SiO_2 49–54 wt.%). In fact, using more anorthitic plagioclase, such as that analyzed as megacrysts in the AGGD ($An_{56}Or_3$) worked better, with lower residuals. It is considered unlikely that the apparent changes in bulk composition and mineral chemistry could be explained by rapidly changing conditions in a source region during partial melting, and crystal fractionation can be justified by, for example, the phenocrysts or early-formed crystals present. The change in mineral assemblage controlling the trends, i.e.,

for Eu^{2+} over the other (trivalent) REE (e.g., Cox et al., 1979). Removal of plagioclase from a silicate melt therefore tends to leave a melt with REE relatively depleted in Eu. Partial melts derived from a source with residual plagioclase will suffer similar depletion of Eu^{2+}. Experiments have shown that Sr, and by analogy Eu^{2+}, are less concentrated by apatite than are the trivalent REE; although Sr is still greater in apatite than the coexisting silicate liquids (Watson and Green, 1981). Only under unusually oxidizing conditions would apatite have no Eu-anomaly (Watson and Green, 1981) and the relatively apatite-rich larvikites have low measured Fe^{3+}/Fe^{2+} whole-rock values (Table 2). Thus, apatite removal from a melt could enrich the melt in Eu^{2+} and potentially generate a positive Eu-anomaly. Extraction of both plagioclase and apatite, as deduced from the whole rock chemistry for SM5, would have opposite effects on the Eu-anomaly of the derivative melts. Extraction of both minerals would successfully remove Sr, but the transition from a positive Eu-anomaly to a negative Eu-anomaly implies that plagioclase had the dominant role. This leaves the problem of the initial positive Eu-anomaly in the erly larvikites of SM5. An interesting, but speculative explanation is provided by the Motzfeldt data and rests on the observation of plagioclase cores, irregularly mantled by alkali feldspar in the larvikites. We suggest that the positive Eu-anomalies resulted directly from large scale incorporation of pre-existing feldspar-rich cumulates. Such early-formed Ol- and Pl-rich cumulates from deeper levels would have contained relatively anorthite-rich feldspar which would also have been Eu-rich and the observed positive Eu-anomalies could therefore be explained by mixing.

The amount of heat required for assimilation of existing crystalline material would have been large, but could have been derived partly from contemporaneous heat of crystallization and in any case the plagioclase cores indicate that the material was not completely melted. The large amount of heat involved would also be intuitively consistent with the tendency towards increasing basicity of successive magmas. Excluding the lujavrites, whose relative age is not well constrained, the last major syenite unit SM5, crystallized from the most basic syenite magmas at Motzfeldt, namely the larvikites. In a sense, this basic trend was continued in the form of the later AGGD which cuts SM5 (Fig. 1) and carries plagioclase megacrysts (Emeleus and Harry, 1970; Jones, 1980). A similar trend of increasing basicity with time has been noted for other centers in the Gardar province (e.g., Stephenson, 1976) and the common association of plagioclase megacrysts with many of the basic dikes was the subject of a lengthy study by Bridgwater and Hary (1968). In view of the late intrusion of the lardalites in the history of the Oslo alkaline province, it is possible that their positive Eu-anomalies could also have resulted from incorporation of earlier plagioclase-rich cumulates. A mechanism of partial melting was considered by Neumann (1980) to be unlikely, but a combination of assimilation followed by fractional crystallization could explain their basic chemistry combined with relatively high

Table 5. Proposed hierarchy of obvious accessory REE-bearing minerals

Note : - see also Jones (1984) for general crystallisation scheme.

incompatible element and REE contents with positive Eu-anomalies.

REE-minerals

Given the range in the degree of fractionation of the syenite samples (Table 2; D.I 59 to 93) and two orders of magnitude reduction in Sr, Ba and Sc, it is perhaps surprising that the variations in REE are so modest (Table 3). This is probably because the REE do not represent truly incompatible elements and were not simply concentrated in shrinking amounts of residual magmas. Therefore, bulk distribution coefficients (K_D's) for the REE were probably near 1.0 in the Motzfeldt syenites, and were similarly close to unity in the Oslo larvikites (Neumann, 1980, p. 516). Several different minerals were responsible for extraction of the REE from the syenite magmas (Table 5) and their REE patterns might give information about the geochemistry of the evolving magmas; they might also record the effects of metasomatism.

The expected light REE-enriched patterns for apatite and sphene (not shown) in the less-fractionated syenites are partly counterbalanced by the role of zircon, which is heavy REE-rich. With the exception of the positive Eu-anomalies, the REE in the basic syenites might be rationalized in terms of different admixtures of apatite, sphene and zircon. In reality, of course, some REE are also distributed as trace elements throughout the major rock-forming minerals. Calculations based on the distribution of La between known modal minerals and measured whole rock values for a nepheline trachyte dike (Larsen, 1979 and unpublished data), slightly more evolved than the larvikites of SM5, indicate that about half of the trachyte's REE are located in fine-grained accessory minerals. Other REE-bearing minerals in Motzfeldt include melanite garnet and pyrochlore in mafic bands from unit SM1 and pyrochlore in SM6. The role of sphene is apparently replaced by minerals of the lâvenite–rinkite family and it is not surprising that these too are light REE-dominated. The Zr-rich varieties of lâvenite occur primarily in syenites devoid of zircon, which may explain their flatter REE patterns (Fig. 6, AM51).

The principal Zr-mineral changes from zircon to eudialyte in the peralkaline syenites, possibly reflecting increasing availability of alkalies and volatile species. The eudialyte shows light REE-enrichment but also has a

Fig. 7. Chondrite-normalized REE distributions for the lujavrites (unit SM6, 46261) from Motzfeldt compared with the hypothetical parental magma for the Ilímaussaq intrusion (Larsen, 1979).

kinked pattern due to some heavy REE. It is possible that most of the REE which would have been present in zircon, are instead accomodated in eudialyte in the more fractionated syenites. Thus, there is a strong and expected correlation between the probe-measured REE in eudialyte and the INAA-measured whole-rock analyses of the lujavrites (Fig. 6), whose primary REE host is eudialyte. Similar comparisons between probe analyses of dominant REE-minerals and host rock REE exist between perovskite and kimberlite (Jones and Wyllie, 1984).

Development of lujavrite

Field evidence shows that the lujavrites intruded earlier syenites and behaved as magmas (Jones, 1980). The simplest interpretation is that the lujavrites are late-stage products derived by extensive fractionation of the syenite magmas of unit SM1 or SM4, and they were emplaced at a high structural level. Their remarkably high Zr contents are consistent with experimental results and are taken to be due to complexing of dissolved Zr^{4+} with "free" alkalies not associated with Al in the melt; a natural consequence of peralkalinity (Watson, 1979; Watson and Harrison, 1983). In terms of their chemistry, mineralogy and occurrence, the lujavites (SM6) from Motzfeldt are comparable with lujavrites and other agpaitic rocks in the Ilímaussaq Intrusion, S. Greenland (Ferguson, 1964; Bailey et al., 1978) and in Lovozero, U.S.S.R. (Vlasov et al., 1966; Gerasimovsky and Kusnetsova, 1967). The SM6 lujavrites are somewhat coarser-grained than their counterparts in Ilímaussaq, and have geochemical affinities with kakortokites from the latter intrusion (Ferguson, 1964). Likely ranges for the REE content of the initial magma to the Ilímaussaq Intrusion (?olivine–phonolite) were estimated

by Larsen (1979) and these are remarkably similar to the dark lujavrite (46261) of SM6 from Motzfeldt, as shown in Figure 7. The euhedral outlines and petrographic textures of eudialyte in fractionated syenites from the central regions of SM5 (Jones, 1980) suggest that eudialyte just achieved the status of a cumulus mineral at Motzfeldt. It seems reasonable that extrapolation of this process could have led to the formation of layered cumulate eudialyte-syenites similar to those so well displayed in the Ilímaussaq Intrusion (Ferguson, 1970). The lujavrites at Ilímaussaq are late-stage products, just as in Motzfeldt, and future comparative work between the two occurrences might be very useful, although it is beyond the scope of this paper.

Metasomatism

Evidence for metasomatic fluids is seen in the lujavrites in the form of replacement of eudialyte by catapleiite and other minerals. On a more widespread basis, syenites from elsewhere in the center show nepheline replaced by sodalite and cancrinite, with the development of albitic rims to perthites. By analogy with experimentally-derived stability limits of sodalite in aqueous syenite systems (Wellman, 1970) these replacement textures are interpreted to have resulted from metasomatism by aqueous fluids. These fluids may have affected whole rock Zr/Ce and Zr/Yb ratios, and might even have been responsible for some growth of rinkite minerals. The fairly common replacement of nepheline by natrolite may also be related to the same fluids.

Given that metasomatic fluids were widely available in the Motzfeldt syenites, especially in the roof zones, then the sample of altered SM1 syenite (63760) becomes particularly interesting. This sample is enriched in many of the same elements found in the lujavrites, notably Zn and Pb (Table 3), and is even more enriched in Nb and Ta, due to the presence of Nb-astrophyllite. The REE, including the negative Eu-anomaly, are also quite similar to the lujavrites (Fig. 3). This suggests that the metasomatic fluids, although not necessarily contemporaneous, have apparently enriched some of the normal syenites with the same elements that are characteristic of the lujavrites. The origin of the lujavrites was not metasomatic, as outlined above, but it should be noted that the processes of late stage igneous enrichment and metasomatic fluids are not mutually exclusive, and may of course be related.

Summary

The following petrogenesis of the center has been proposed above:

(1) Sr isotopic evidence suggests an ultimate mantle source and the most basic magma available was alkali gabbro (Ti-rich olivine-basalt) seen in the late giant dike (AGGD). Alkali gabbro, larvikites and nepheline syenites can be related by progressive removal of Ol + Pl at deeper levels followed by Ol + Pl + Cpx ± Amph at current levels of exposure.

(2) Positive Eu-anomalies in the larvikites have been explained by incorporation of earlier plagioclase-rich cumu-

lates and are seen as plagioclase relics. This could be tested since plagioclase separates from the larvikites, and probably from the AGGD should have substantial positive Eu-anomalies.

(3) The lujavrites are late-stage products derived by extensive fractionation of nepheline syenites, either of unit SM1 or SM4.

(4) Metasomatic fluids apparently affected many of the syenites and have geochemical signatures similar to the late-stage lujavrites. A related origin is implied but more work is needed.

This scheme is in general agreement with the widely accepted view of parental augite syenite (similar to SM5 lar-vikites) to many of the Gardar centers, and emphasizes the importance of giant dikes such as those of transitional olivine basalt from Tugtutôq (Upton and Thomas, 1980), in the Gardar province. The unexpectedly high positive Eu-anomalies and the apparent significance of plagioclase lead back to the ideas of Bridgwater and Harry (1968), which seem to warrant renewed interest.

References

Allart, J. (1973) Geological map of Greenland 1:100,000. Juliane-haab 60V.2Nord descriptive text. Grønlands geologiske Undersøgelse, Copenhagen.

Bailey, J. C., Larsen, L. M. and Sørenson, H. (1981) Introduction to the Ilímaussaq intrusion with a summary of the reported investigations. Rapport Grønlands geologiske Undesrøgelse, 103, 5–17.

Bailey, J. C., Gwozdz, R., Rose-Hansen, J. and Sørenson, H. (1978) Preliminary geochemical work on the Ilímaussaq alkaline intrusion, South Greenland. Rapport Grønlands geologiske Undersøgelse, 90, 75–79.

Blaxland, A. B., van Breeman, O., Emeleus, C. H. and Anderson, J. G. (1978) Age and origin of the major syenite centres in the Gardar province of South Greenland: Rb–Sr studies. Bulletin of the Geological Society of America, 89, 231–244.

Bridgwater, D. and Harry, W. T. (1968) Anorthosite xenoliths and plagioclase megacrysts in Precambrian intrusions of South Greenland. Meddelelser om Grønland, 185, 1–66.

Chambers, A. D. (1976) The petrology and mineralogy of the North Qôroq Centre, Igaliko Complex, South Greenland. Unpubl. Ph.D. thesis, University of Durham.

Cox, K. G., Bell, J. D. and Pankhurst, R. J. (1979) The interpretation of igneous rocks. George Allen and Unwin, London.

Davis, A. M., Tanaka, T., Grossman, L., Lee, T. and Wasserburg, G. J. (1982) Chemical composition of HAL, an isotopically unusual Allende inclusion. Geochimica et Cosmochimica Acta, 46, 1627–1651.

Emeleus, C. H. and Harry, W. T. (1970) The Igaliko nepheline syenite complex. General Description. Meddelelser om Grøn-land, 186, also Bulletin Grønlands geologiske Under-søgelse, 85.

Emeleus, C. H. and Upton, B. G. J. (1976) The Gardar period in southern Greenland. In A. Escher and W. S. Watt, Eds., The Geology of Greenland, p. 152–181. Geological Survey of Greenland, Copenhagen.

Exley, R. A. (1980) Microprobe studies of REE-rich accessory minerals: implications for Skye granite petrogenesis and REE mobility in hydrothermal systems. Earth and Planetary Science Letters, 48, 97–110.

Ferguson, J. (1964) Geology of the Ilímaussaq alkaline intrusion, South Greenland. Meddelelser om Grønland, 172, also Bulletin Grønlands geologiske Undersøgelse, 89.

Ferguson, J. (1970) The differentiation of agpaitic magmas: the Ilímaussaq Intrusion, South Greenland. Canadian Mineralogist, 10, 335–349.

Fleischer, M. (1978) Relation of the relative concentrations of lanthanides in titanite to type of host rocks. American Mineralogist, 63, 869–873.

Galli, E. and Alberti, A. (1971) The crystal structure of rinkite. Acta Crystallographica, B27, 1277–1284.

Gerasimovsky, V. I. and Kusnetsova, S. Ya. (1967) On the petrochemistry of the Ilímaussaq intrusion, South Greenland. Geochemistry International, 4, 236–246.

Giradi, F., Guzzi, G. and Pauly, J. (1965) Reactor neutron activation analysis by the single comparator method. Analytical Chemistry, 37, 1085–1092.

Hamilton, D. L. (1961) Nephelines as crystallisation temperature indicators. Journal of Geology, 69, 321–329.

Henderson, P. (1980) Rare earth element partitioning between sphene, apatite and other coexisting minerals of the Kangerd-lugssuaq intrusion, E. Greenland. Contributions to Mineralogy and Petrology, 72, 81–85.

Jones, A. P. (1980) The petrology and structure of the Motzfeldt Centre, Igaliko, South Greenland. Unpubl. Ph.D. thesis, University of Durham.

Jones, A. P. (1984) Mafic silicates from the nepheline syenites of the Motzfeldt Centre, South Greenland. Mineralogical Magazine, 48, 1–12.

Jones, A. P. and Ekambaram, V. (1985) New INAA analysis of a mantle-derived titanate mineral of the crichtonite series, with particular reference to the rare earth elements. American Mineralogist, 70, 414–418.

Jones, A. P. and Peckett, A. (1980) Zirconium-bearing aegirines from the Motzfeldt Centre, South Greenland. Contributions to Mineralogy and Petrology, 75, 251–255.

Jones, A. P. and Wyllie, P. J. (1984) Minor elements in perovskite from kimberlites and distribution of the rare earth elements: an electron probe study. Earth and Planetary Science Letters, 69, 128–140.

Larsen, L. M. (1979) Distribution of REE and other trace elements between phenocrysts and peralkaline undersaturated magmas, exemplified by rocks from the Gardar igneous province, south Greenland. Lithos, 12, 303–315.

Larsen, L. M. (1981) Chemistry of feldspars in the ilímaussaq augite syenite with additional data on some other minerals. Rapport Grønlands geologiske Undersøgelse, 103, 31–37.

Nakamura, N. (1974) Determination of REE, Ba, Fe, Mg, Na and K in carbonaceous chondrites. Geochimica et Cosmochimica Acta, 38, 757–775.

Neumann, E.-R. (1980) Petrogenesis of the Oslo region larvikites and associated rocks. Journal of Petrology, 21, 499–531.

Patchett, P. J., Hutchinson, J., Blaxland, A. B. and Upton, B. G. J.

(1976) Origin of anorthosites, gabbros and potassic ultramafic rocks from the Gardar province, south Greenland: initial $^{87}Sr/^{86}Sr$ studies. Bulletin of Geological Society of Denmark, 25, 79–84.

Powell, M. and Powell, R. (1977) A nepheline-alkali feldspar geothermometer. Contributions to Mineralogy and Petrology, 62, 193–204.

Sørenson, H. (1969) Rhythmic igneous layering in peralkaline intrusions. An essay review on Ilímaussaq (Greenland) and Lovozero (Kola, USSR) Lithos, 2, 261–283.

Stephenson, D. (1976) The South Qôroq Centre nepheline syenites, South Greenland: petrology, felsic mineralogy and petrogenesis. Bulletin Grønlands geologiske Undersøgelse, 118.

Sun, S-S. and Hanson, G. N. (1975) Rare earth element evidence for differentiation of McMurdo volcanics, Ross Island, Antarctica. Contributions to Mineralogy and Petrology, 54, 139–155.

Thornton, C. P. and Tuttle, O. F. (1960) Chemistry of igneous rocks: 1, differentiation index. American Journal of Science, 252, 67–75.

Tukiainen, T., Bradshaw, B. and Emeleus, C. H. (1984) Geological and radiometric mapping of the Motzfeldt Centre of the Igaliko Complex, South Greenland. Rapport Grønlands geologiske Undersøgelse, 120, 78–83.

Upton, B. G. J. (1964) The geology of Tugtutôq and neighbouring islands, South Greenland. Bulletin Grønlands geologiske Undersøgelse, 48; also Meddelelser om Grønland, 169.

Upton, B. G. J. and Thomas, J. E. (1980) The Tugtutôq Younger Giant Dyke Complex, South Greenland: fractional crystallization of transitional olivine basalt magma. Journal of Petrology, 21, 167–198.

Vlasov, K. A., Kuz'menko, M. V. and Eskova, E. M. (1966) The Lovozéro alkaline massif. Oliver and Boyd, Edinburgh and London.

Watson, E. B. (1979) Some experimentally determined zircon/liquid partition coefficients for the rare earth elements. Geochimica et Cosmochimica Acta, 44, 895–897.

Watson, E. B. and Green, T. H. (1981) Apatite/liquid partition coefficients for the rare earth elements and strontium. Earth and Planetary Science Letters, 56, 405–421.

Watson, E. B. and Harrison, T. M. (1983) Zircon saturation revisited: temperature and composition effects in a variety of crustal magma types. Earth and Planetary Science Letters, 64, 295–304.

Wellman, T. R. (1970) The stability of sodalite in a synethetic syenite plus aqueous chloride fluid system. Journal of Petrology, 11, 49–71.